

# Structures and Biosynthetic Pathway of Coprisamides C and D, 2-Alkenylcinnamic Acid-Containing Peptides from the Gut Bacterium of the Carrion Beetle *Silpha perforata*

Yern-Hyerk Shin, Yeon Hee Ban, Tae Ho Kim, Eun Seo Bae, Jongheon Shin, Sang Kook Lee, Jichan Jang, Yeo Joon Yoon, and Dong-Chan Oh\*



Cite This: *J. Nat. Prod.* 2021, 84, 239–246



Read Online

ACCESS |



Metrics & More

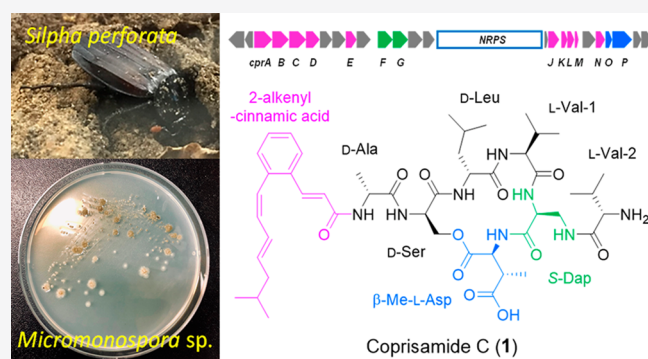


Article Recommendations



Supporting Information

**ABSTRACT:** Coprisamides C and D (**1** and **2**) were isolated from a gut bacterium, *Micromonospora* sp. UTJ3, of the carrion beetle *Silpha perforata*. Based on the combined analysis of UV, MS, and NMR spectral data, the planar structures of **1** and **2** were elucidated to be unreported derivatives of coprisamides A and B, cyclic depsipeptides bearing a 2-alkenylcinnamic acid unit and the unusual amino acids  $\beta$ -methylaspartic acid and 2,3-diaminopropanoic acid. The absolute configuration of **1** was determined using the advanced Marfey's method, phenylglycine methyl ester derivatization, and *J*-based configuration analysis. The biosynthetic gene clusters for the coprisamides were investigated based on genomic data from coprisamide-producing strains *Micromonospora* sp. UTJ3 and *Streptomyces* sp. SNU533. Coprisamide C (**1**) was active against the *Mycobacterium tuberculosis* mc<sup>2</sup> 6230 strain.



Microorganisms that inhabit the guts of insects, which depend on the species, as well as habitats and food sources, are proven sources for new bioactive natural products.<sup>1</sup> Coprisamides A and B were discovered from a dung beetle gut bacterium in 2015,<sup>2</sup> which provided the first evidence of the great chemical potential of these hidden bacterial communities, and subsequent studies of insect gut bacteria further revealed structurally and biologically interesting natural products. Additional examples include rubterolones (tropolone-containing antimicrobial alkaloids isolated from the gut of the fungus-growing termite *Macrotermes natalensis*),<sup>3</sup> coprisidins (quinone oxidoreductase-inducing alkaloids with a novel naphthoquinone–oxindole framework from dung beetle-associated *Streptomyces*),<sup>4</sup> bombyxamycins (cytotoxic macrocyclic lactams from the silkworm gut *Streptomyces*),<sup>5</sup> and the gut-bacterial communities of carpenter ants *Camponotus japonicus* and *C. kiusiuensis*, which produce the aminoglycolipids deinococcucins<sup>6</sup> and the polyketide alkaloids camporidines.<sup>7</sup> Therefore, an expanded investigation of a broader range of more diverse insects should be an effective strategy for discovering novel bioactive compounds.

Studies on the microbial community profiles of carrion beetles in the Silphidae family showed that these insects harbor abundant and distinctive hindgut communities, including chemically prolific actinobacteria.<sup>8</sup> Carrion beetles can be classified into two subfamilies, i.e., Nicrophorinae and Silphinae.<sup>9</sup> It was reported that a rare actinomycete, *Micro-*

*bacterium* sp., present in the gut of the beetle *Nicrophorus concolor* (Nicrophorinae subfamily) produced the antibacterial chlorinated cyclic hexapeptides nicrophorusamides A and B.<sup>10</sup> To date, microbes associated with the *Silpha* genus in the Silphinae subfamily have not been well investigated chemically. Indeed, only chemical reports of the production of defensive steroids from the rectal glands of *S. noveboracensis* and *S. americana* have been reported.<sup>11,12</sup> Members of the Silphinae subfamily, which comprises flightless roving carrion beetle species,<sup>13</sup> usually feed on soil invertebrates, whereas Nicrophorinae members feed on vertebrate carcasses.<sup>14</sup> On the basis of these findings, we chose to focus on the gut bacteria of *Silpha perforata*, a species of the Silphinae subfamily.

Herein, we report results of chemical profiling of a gut bacterium, *Micromonospora* sp. UTJ3, from *S. perforata* through LC/MS analysis to detect the production of unidentified secondary metabolites. Spectroscopic analysis was employed to elucidate the planar structures of the unknown compounds, named coprisamides C and D, and to relate them to the

Received: August 3, 2020

Published: January 26, 2021

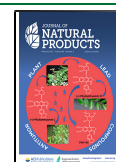


Table 1. <sup>1</sup>H and <sup>13</sup>C NMR Spectral Data of Coprisamides C and D (1 and 2) in DMSO-*d*<sub>6</sub>

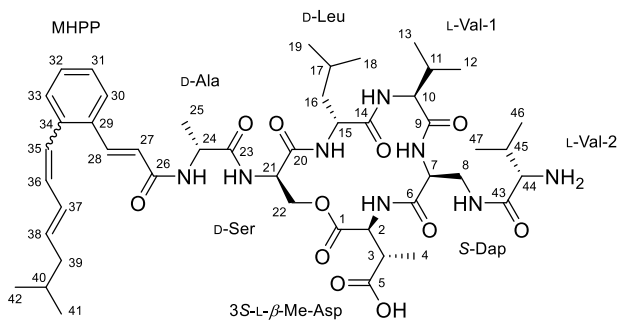
no.	coprisamide C <sup>a</sup> (1)				coprisamide D <sup>b</sup> (2)			
	δ <sub>C</sub>	type	δ <sub>H</sub>	mult (J in Hz)	δ <sub>C</sub>	type	δ <sub>H</sub>	mult (J in Hz)
1	169.5	C			169.5	C		
2	54.7	CH	3.82	dd (10.5, 7.5)	54.7	CH	3.81	dd (10.5, 7.5)
2-NH			8.51	d (7.5)			8.55	d (7.5)
3	38.6	CH	2.98	dq (10.5, 7.5)	38.6	CH	2.98	dq (10.5, 7.5)
4	14.9	CH <sub>3</sub>	0.98	d (7.5)	14.9	CH <sub>3</sub>	0.98	d (7.5)
5	176.0	C			176.0	C		
6	169.2	C			169.2	C		
7	49.9	CH	4.68	ddd (9.5, 9.5, 5.0)	49.9	CH	4.69	ddd (9.5, 9.5, 4.5)
7-NH			8.15	d (9.5)			8.16	d (9.5)
8a	39.2	CH <sub>2</sub>	4.01	m	39.2	CH <sub>2</sub>	4.02	m
8b			2.89	m			2.88	m
8-NH			8.57	dd (7.5, 4.0)			8.52	dd (6.5, 4.5)
9	170.3	C			170.3	C		
10	58.0	CH	4.24	dd (9.0, 4.0)	58.0	CH	4.24	dd (9.0, 4.0)
10-NH			8.39	d (9.0)			8.39	d (9.0)
11	28.1	CH	2.38	m	28.1	CH	2.38	m
12	16.8	CH <sub>3</sub>	0.84	d (7.0)	16.8	CH <sub>3</sub>	0.85	d (7.0)
13	16.8	CH <sub>3</sub>	0.84	d (7.0)	16.8	CH <sub>3</sub>	0.85	d (7.0)
14	172.7	C			172.7	C		
15	52.9	CH	4.28	m	52.9	CH	4.29	m <sup>c</sup>
15-NH			8.73	d (4.0)			8.73	d (4.0)
16a	38.8	CH <sub>2</sub>	1.56	m	39.0	CH <sub>2</sub>	1.56	m
16b			1.41	ddd (14.0, 7.0, 7.0)			1.41	ddd (13.0, 7.0, 7.0)
17	24.2	CH	1.50	m	24.2	CH	1.51	m
18	22.8	CH <sub>3</sub>	0.92	d (7.0)	22.8	CH <sub>3</sub>	0.87	d (6.5)
19	21.9	CH <sub>3</sub>	0.86	d (7.0)	21.9	CH <sub>3</sub>	0.87	d (6.5)
20	169.7	C			169.7	C		
21	50.5	CH	4.50	ddd (7.5, 3.0, 2.0)	50.7	CH	4.51	ddd (7.5, 2.5, 2.5)
21-NH			7.32	d (7.5)			7.34	d (7.5)
22a	63.2	CH <sub>2</sub>	4.89	dd (11.0, 3.0)	63.4	CH <sub>2</sub>	4.91	dd (11.0, 2.5)
22b			3.96	dd (11.0, 2.0)			3.97	dd (11.0, 2.5)
23	171.5	C			171.5	C		
24	49.4	CH	4.27	qd (7.0, 7.0)	49.5	CH	4.30	m <sup>c</sup>
24-NH			8.01	d (7.0)			8.03	d (7.0)
25	17.4	CH <sub>3</sub>	1.31	d (7.0)	17.4	CH <sub>3</sub>	1.33	d (7.0)
26	164.5	C			164.5	C		
27	122.8	CH	6.91	d (15.5)	123.5	CH	6.87	d (15.5)
28	137.0	CH	7.57	d (15.5)	136.5	CH	7.78	d (15.5)
29	133.3	C			132.4	C		
30	130.0	CH	7.24	d (7.5)	126.5	CH	7.52	d (7.5)
31	129.0	CH	7.38	dd (7.5, 7.5)	127.5	CH	7.25	dd (7.5, 7.5)
32	127.6	CH	7.31	dd (7.5, 7.5)	129.5	CH	7.35	dd (7.5, 7.5)
33	126.3	CH	7.61	d (7.5)	126.0	CH	7.59	d (7.5)
34	136.9	C			136.6	C		
35	125.6	CH	6.48	d (11.5)	126.1	CH	6.80	d (15.5)
36	131.9	CH	6.40	dd (11.5, 11.5)	132.6	CH	6.78	dd (15.5, 9.0)
37	126.9	CH	6.12	dd (15.0, 11.5)	131.8	CH	6.32	dd (15.0, 9.0)
38	137.1	CH	5.91	dt (15.0, 7.5)	135.5	CH	5.91	dt (15.0, 7.5)
39	41.6	CH <sub>2</sub>	1.91	dd (7.5, 7.5)	41.6	CH <sub>2</sub>	2.03	dd (7.5, 7.5)
40	27.9	CH	1.60	m	28.0	CH	1.67	m
41	22.1	CH <sub>3</sub>	0.83	d (7.0)	22.2	CH <sub>3</sub>	0.89	d (6.5)
42	22.1	CH <sub>3</sub>	0.83	d (7.0)	22.2	CH <sub>3</sub>	0.89	d (6.5)
43	168.0	C			167.9	C		
44	57.6	CH	3.56	m	57.6	CH	3.53	m
44-NH <sub>2</sub>			8.11	d (4.5)			8.07	d (4.5)
45	29.8	CH	2.03	m	29.8	CH	2.03	m <sup>c</sup>
46	18.4	CH <sub>3</sub>	0.91	d (6.5)	18.4	CH <sub>3</sub>	0.92	d (6.5)
47	17.2	CH <sub>3</sub>	0.87	d (6.5)	17.2	CH <sub>3</sub>	0.88	d (6.5)

<sup>a</sup><sup>1</sup>H 850 MHz, <sup>13</sup>C 212.5 MHz. <sup>b</sup><sup>1</sup>H 800 MHz, <sup>13</sup>C 200 MHz. <sup>c</sup>Overlapping.

compounds (coprisamides A and B) previously isolated from the gut bacterium *Streptomyces* sp. SNU533 of the dung beetle *Copris tripartitus*.<sup>2</sup> Coprisamide C exhibited weak activity against a strain of *Mycobacterium tuberculosis* (Mtb). The biosynthetic pathways were elucidated by performing comparative analysis of two coprisamide-producing bacterial strains, *Streptomyces* sp. SNU533 and *Micromonospora* sp. UTJ3.

## RESULTS AND DISCUSSION

Coprisamide C (**1**) was acquired as a white powder by chromatographic purifications. The unsaturation number of **1** was calculated to be 17 by the molecular formula (C<sub>47</sub>H<sub>70</sub>N<sub>8</sub>O<sub>11</sub>), which was determined by high-resolution electrospray ionization mass spectrometry (HR-ESIMS) data coupled with <sup>1</sup>H and <sup>13</sup>C NMR spectroscopic data (Table 1). Further analysis of the <sup>1</sup>H NMR spectrum of coprisamide C (**1**), as well as HSQC NMR spectroscopic data, indicated the existence of nine amide hydrogens ( $\delta_{\text{H}}$  7.32, 8.01, 8.11 (2H), 8.15, 8.39, 8.51, 8.57, and 8.73), six olefinic methine hydrogens ( $\delta_{\text{H}}$  5.91, 6.12, 6.40, 6.48, 6.91, and 7.57), and four aromatic hydrogens ( $\delta_{\text{H}}$  7.24, 7.31, 7.38, and 7.61) in the downfield region, based on their chemical shifts and <sup>3</sup>J<sub>HH</sub> values (olefinic hydrogens: <sup>3</sup>J<sub>HH</sub> = 11.5–15.0 Hz; aromatic hydrogens: <sup>3</sup>J<sub>HH</sub> = 7.5 Hz). Furthermore, seven  $\alpha$ -amino methine hydrogen signals were detected at  $\delta_{\text{H}}$  3.5–4.7 ( $\delta_{\text{H}}$  3.56, 3.82, 4.24, 4.27, 4.28, 4.50, and 4.68), suggesting that coprisamide C (**1**) contained seven amino acid units in its structure. The <sup>13</sup>C NMR spectrum of **1** showed signals corresponding to nine carbonyl carbon atoms ( $\delta_{\text{C}}$  164.5, 168.0, 169.2, 169.5, 169.7, 170.3, 171.5, 172.7, and 176.0) and 12 sp<sup>2</sup> carbon atoms ( $\delta_{\text{C}}$  122.8, 125.6, 126.3, 126.9, 127.6, 129.0, 130.0, 131.9, 133.3, 136.9, 137.0, and 137.1), which accounted for 15 out of the 17 double-bond equivalents of coprisamide C (**1**). This result revealed that coprisamide C (**1**) is a bicyclic compound. In addition, we detected carbon signals corresponding to one oxygen-bound carbon atom ( $\delta_{\text{C}}$  63.2) and seven carbon atoms at the  $\alpha$ -positions of the amino acids ( $\delta_{\text{C}}$  49.4, 49.9, 50.5, 52.9, 54.7, 57.6, and 58.0).



1: 35Z, 2: 35E

All one-bond <sup>1</sup>H–<sup>13</sup>C correlations were assigned by interpreting the HSQC NMR spectrum with the <sup>1</sup>H and <sup>13</sup>C NMR spectroscopic data (Table 1). Combinational analysis of the COSY, HMBC, and TOCSY NMR data revealed that coprisamide C (**1**) possessed five common amino acids (alanine, serine, leucine, and two valine residues) and two non-proteinogenic amino acid units, including  $\beta$ -methylaspartic acid ( $\beta$ -Me-Asp) and 2,3-diaminopropanoic acid (Dap). Initially, the C-4–C-3–C-2–2-NH connectivity was constructed via sequential COSY/TOCSY correlations, and their HMBC correlations indicated that carbonyl carbon atoms C-1 ( $\delta_{\text{C}}$  169.5) and C-5 ( $\delta_{\text{H}}$  176.0) were likely connected to C-2 ( $\delta_{\text{C}}$

54.7) and C-3 ( $\delta_{\text{C}}$  38.6), respectively, suggesting that the amino acid unit was a  $\beta$ -Me-Asp (Figure 1). An array of <sup>1</sup>H–<sup>1</sup>H COSY/

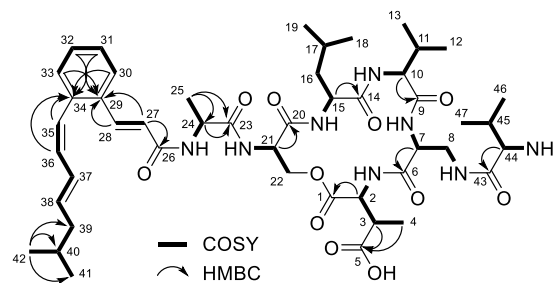
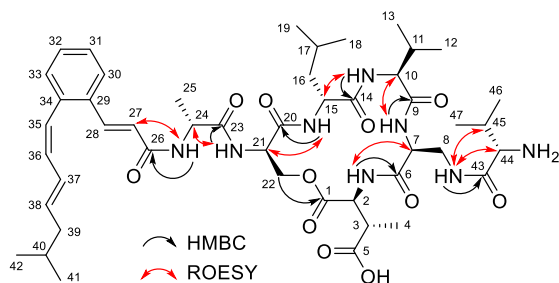


Figure 1. Key COSY and intraunit HMBC correlations used for determining the structure of coprisamide C (**1**).

TOCSY correlations revealed connectivity from 7-NH ( $\delta_{\text{H}}$  8.15) to 8-NH ( $\delta_{\text{H}}$  8.57), and the carbonyl carbon atom C-6 ( $\delta_{\text{C}}$  169.2) was linked to C-7 ( $\delta_{\text{C}}$  49.9) based on a <sup>1</sup>H–<sup>13</sup>C HMBC correlation from H-7 ( $\delta_{\text{H}}$  4.68) to C-6, confirming that this amino acid was a Dap unit (Figure 1). The proteinogenic amino acid residues present in **1**, two valines (Val-1 and Val-2), leucine (Leu), serine (Ser), and alanine (Ala), were also identified by comprehensive analysis of the 1D and 2D NMR spectral data.

The final moiety that was responsible for the UV spectral absorption ( $\lambda_{\text{max}}$  267 and 288 nm) was identified based on the COSY, TOCSY, and HMBC NMR spectra. TOCSY correlations indicated that three discrete spin systems were present in this substructure. One of the spin systems was identified as C-27–C-28 by a COSY correlation between H-27 ( $\delta_{\text{H}}$  6.91) and H-28 ( $\delta_{\text{H}}$  7.57). An array of <sup>1</sup>H–<sup>1</sup>H correlations of H-30, H-31, H-32, and H-33 ( $\delta_{\text{H}}$  7.24, 7.38, 7.31, and 7.61, respectively) and their <sup>1</sup>H–<sup>1</sup>H coupling constants (7.5 Hz) revealed that another spin system constituted a six-membered aromatic ring. Furthermore, fully substituted carbon atoms (C-29 and C-34) comprising the aromatic structure were assigned by the HMBC NMR data. More specifically, based on HMBC correlations from H-30/H-32 to C-34 ( $\delta_{\text{C}}$  136.9) and from H-31/H-33 to C-29 ( $\delta_{\text{C}}$  133.3), along with the C-30–C-31–C-32–C-33 spin system, a six-membered aromatic ring structure was established. The last spin system was successfully constructed from H-35 ( $\delta_{\text{H}}$  6.48) to H<sub>3</sub>-42 ( $\delta_{\text{H}}$  0.83) by the consecutive COSY correlations among these hydrogens. HMBC correlations from H<sub>3</sub>-42 ( $\delta_{\text{H}}$  0.83) to C-39 ( $\delta_{\text{C}}$  41.6), C-40 ( $\delta_{\text{C}}$  27.9), and C-41 ( $\delta_{\text{C}}$  22.1) revealed the terminal dimethyl structure. These three spin systems were then assembled through <sup>1</sup>H–<sup>13</sup>C two- or three-bond correlations. In this case, an HMBC signal from H-27 to C-26 ( $\delta_{\text{C}}$  164.5) elucidated that the carbonyl carbon atom C-26 was linked to C-27 ( $\delta_{\text{C}}$  122.8), whereas HMBC correlations from H-27/H-28 to C-29 and from H-35/H-36 ( $\delta_{\text{H}}$  6.40) to C-34 finally disclosed the last partial structure, 3-[2-(6-methyl-1,3-heptenyl)phenyl]-2-propenoic acid (MHPP), a 2-alkenylcinnamic acid (Figure 1).

The connections between the partial structures were subsequently elucidated through two- or three-bond <sup>1</sup>H–<sup>13</sup>C couplings (Figure 2). More specifically, 2-NH/C-6, 7-NH/C-9 ( $\delta_{\text{C}}$  170.3), 10-NH ( $\delta_{\text{H}}$  8.39)/C-14 ( $\delta_{\text{C}}$  172.7), 15-NH ( $\delta_{\text{H}}$  8.73)/C-20 ( $\delta_{\text{C}}$  169.7), and 21-NH ( $\delta_{\text{H}}$  7.32)/C-23 ( $\delta_{\text{C}}$  171.5) HMBC correlations confirmed the  $\beta$ -Me-Asp–Dap–Val-1–Leu–Ser–Ala amino acid sequence. This sequence was further crosschecked based on ROESY correlations between the amide hydrogens and  $\alpha$ -hydrogens of the amino acid units. The 2-alkenylcinnamic acid unit (MHPP) was found to be connected



**Figure 2.** Determining the amino acid sequence of **1** based on interunit HMBC and ROESY correlations.

to 24-NH ( $\delta_{\text{H}}$  8.01) by an HMBC correlation of 24-NH/C-26 and a ROESY correlation between 24-NH and H-27. The additional Val unit (Val-2) was located adjacent to Dap, as confirmed by the 8-NH/C-43 ( $\delta_{\text{C}}$  168.0) two-bond HMBC correlation. Although no further HMBC correlations were observed, ROESY correlations from 8-NH to the  $\alpha$ - and  $\beta$ -amino hydrogens, i.e., H-44 ( $\delta_{\text{H}}$  3.56) and H-45 ( $\delta_{\text{H}}$  2.03), of Val-2 supported this branched connectivity. Thus, coprisamide C (**1**) was identified as a cyclic depsipeptide containing 2-alkenylcinnamic acid (MHPP) and a branched amino acid unit attached to 2,3-diaminopropanoic acid.

The geometric configurations of the double bonds in MHPP were then identified, based on the  $^3J_{\text{HH}}$  values. By careful analysis of the  $^1\text{H}$  NMR spectrum,  $^3J_{\text{H}_2\text{H}_28}$  and  $^3J_{\text{H}_3\text{H}_38}$  were measured to be 15.5 Hz, whereas  $^3J_{\text{H}_3\text{H}_36}$  was 11.5 Hz. Therefore, these geometries in **1** could be identified as 27*E*, 35*SZ*, and 37*E*, respectively. Finally, the cinnamoyl moiety of **1** was identified as 3-[2-(6-methyl-1-(*Z*)-3-(*E*)-heptenyl)phenyl]-2-(*E*)-propenoic acid.

The absolute configurations of the amino acids present in **1** were determined by adopting the advanced Marfey's method.<sup>15</sup> For this purpose, the acid hydrolysate of **1** was separately derivatized with *L*- and *D*-1-fluoro-2,4-dinitrophenyl-5-alanine amide (*L*- and *D*-FDAA) and subsequently analyzed by LC/MS using a  $\text{C}_{18}$  column (Figure S17). The elution orders of the FDAA derivatives established the amino acid residues in **1** to be *L*- $\beta$ -Me-Asp, *S*-Dap, *L*-Val-1, *D*-Leu, *D*-Ser, *D*-Ala, and *L*-Val-2, respectively (Table S1).

The absolute configuration at the C-3 stereogenic center, located in the  $\beta$ -Me-Asp unit, was assigned through *S*- and *R*-phenylglycine methyl ester (*S*- and *R*-PGME) derivatization<sup>16</sup> and subsequent analysis of the  $^1\text{H}$  and COSY NMR data of the *S*- and *R*-PGME amides (**1a** and **1b**). The obtained  $\Delta\delta_{\text{S-R}}$  values established that the C-3 center of **1** has an *S* configuration (Figure 3), which was further confirmed by *J*-based configuration analysis. Since the  $\alpha$ - and  $\beta$ -amino hydrogens of the  $\beta$ -Me-Asp unit in **1** (i.e., H-2, and H-3) exhibit a large coupling constant ( $^3J_{\text{H}_2\text{H}_3} = 10.5$  Hz), an anti-relationship between H-2 and H-3 was deduced. The rotamer (Figure S22) was then constructed via the H-2/H<sub>3</sub>-4, H<sub>3</sub>-4/2-NH, and 2-NH/H-3

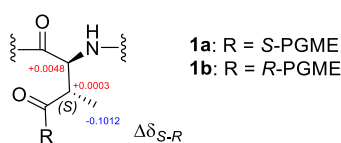


**Figure 3.** Identification of the absolute configuration at C-3, based on the  $\Delta\delta_{\text{S-R}}$  values in ppm of the *S*- and *R*-PGME amides of coprisamide C (**1a** and **1b**).

ROESY correlations. Following the rotamer model, the absolute configuration at C-3 could be deduced as *S* based on the 2*S* configuration, which was determined using the advanced Marfey's method.

Coprisamide D (**2**) was also purified as an amorphous white powder, and the HR-ESIMS data for **2** indicated that it has a molecular formula of  $\text{C}_{47}\text{H}_{70}\text{N}_8\text{O}_{11}$  with an unsaturation number of 17, which is identical to that of **1**. The NMR data for coprisamide D (**2**) and coprisamide C (**1**) were similar (Table 1). The structure of coprisamide D was revealed as a geometric isomer of **1**, which possesses the 3*SE* geometry based on the  $^3J_{\text{H}_3\text{H}_36}$  value (15.5 Hz); this is in contrast to **1**, which possesses the 3*SZ* configuration ( $^3J_{\text{H}_3\text{H}_36} = 11.5$  Hz). In addition, the circular dichroism (CD) spectra of **1** and **2** (Figure S23) were essentially identical, and their common biosynthetic origins revealed that the absolute configurations of the amino acid units in **1** and **2** are the same.

Coprisamides C and D (**1** and **2**) are structurally similar to coprisamides A and B, previously reported from a gut bacterium (*Streptomyces* sp. SNU533) of the dung beetle, *Copris tripartitus*.<sup>2</sup> The amino acid units in **1** and **2** are identical to those in coprisamides A and B (*L*- $\beta$ -Me-Asp, *S*-Dap, two *L*-Val, *D*-Leu, *D*-Ser, and *D*-Ala), and the structural variations reside in their 2-alkenylcinnamic acid units, the most dominant chromophore of coprisamides, which cause dissimilarities in their UV-absorption spectra. Because coprisamides C and D (**1** and **2**) possess 3-[2-(6-methyl-1,3-heptenyl)phenyl]-2-propenoic acid, whereas coprisamides A and B possess 3-[2-(1,3,5-heptenyl)phenyl]-2-propenoic acid, the UV spectra of coprisamides C and A showed that they have different shapes and  $\lambda_{\text{max}}$  values (267 and 288 nm for coprisamide C versus 282 nm for coprisamide A). Thus, further comprehensive NMR spectroscopic analysis was required to elucidate their planar structures.

Coprisamides A–D were tested for their activity against *Mtb* mc<sup>2</sup> 6230 using resazurin microtiter assays (REMA); coprisamide C (**1**) showed mild growth-inhibitory activity against the test strain ( $\text{MIC}_{50}$  value = 82.8  $\mu\text{g}/\text{mL}$ , Figure S24). Because coprisamides A and B were previously reported to induce quinone reductase (QR) activity,<sup>2</sup> coprisamides C and D (**1** and **2**) were also evaluated for this activity. Coprisamides C and D induced QR activity in cells by 2.4- and 2.3-fold, respectively, at a concentration of 10  $\mu\text{M}$  (Figure S25a and b), whereas coprisamides A and B showed 2.6- and 2.1-fold induction of QR activity at the same concentration.<sup>2</sup> However, unlike coprisamides A and B, compounds **1** and **2** displayed cellular cytotoxicities at higher concentrations (Figure S25c and d). **1** and **2** were inactive against *Staphylococcus aureus*, *Enterococcus faecalis*, *Enterococcus faecium*, *Klebsiella pneumoniae*, *Salmonella enterica*, *Escherichia coli*, *Aspergillus fumigatus*, *Trichophyton rubrum*, *Trichophyton mentagrophytes*, and *Candida albicans*.

Genome sequencing of coprisamides C/D and A/B producers, i.e., *Micromonospora* sp. UTJ3 and *Streptomyces* sp. SNU533, respectively, was carried out. AntiSMASH software (version 5.0)<sup>17</sup> revealed that the biosynthetic genes for coprisamides A/B and C/D are organized identically (Figures 4 and S26). The coprisamide C/D biosynthetic gene cluster was found to consist of two genes encoding modular nonribosomal peptide synthetases (NRPSs), in addition to several putative genes involved in biosynthesizing nonproteinogenic amino acids and the modified cinnamoyl moiety (Figure 4a and Table S4). The NRPSs were identified to be composed of six NRPS modules and were predicted to produce a cyclic hexapeptide,

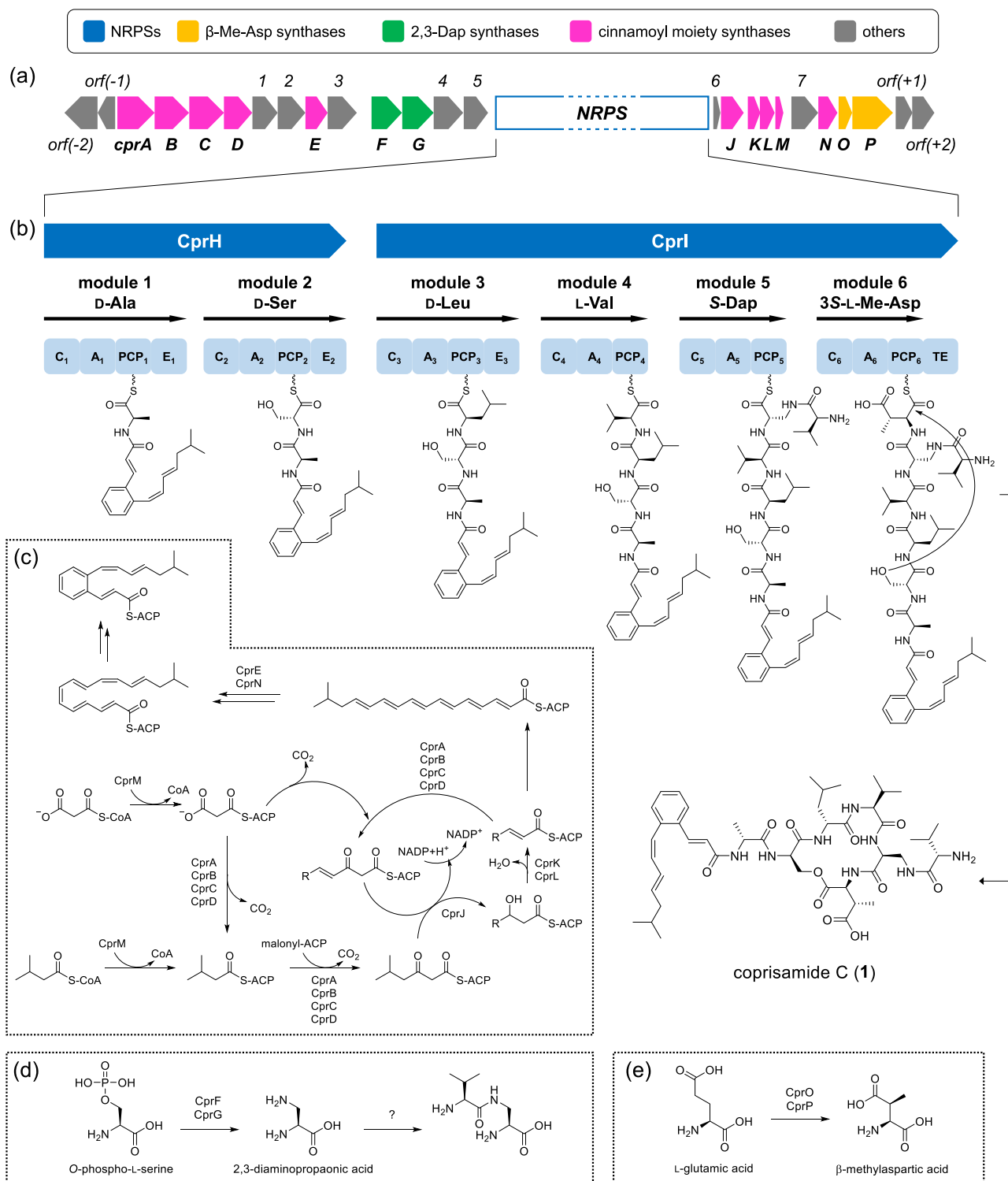


**Figure 4.** (a) Biosynthetic gene cluster for coprisamides C and D. (b) Predicted biosynthetic steps and enzymes used for coprisamide C (1) synthesis. C, condensation domain; A, adenylation domain; PCP, peptide-carrier protein; E, epimerase; TE, thioesterase. (c–e) Predicted biosynthetic pathways for the cinnamoyl moiety, 2,3-diaminopropanoic acid, and  $\beta$ -methylaspartic acid.

which was consistent with the structures of the coprisamides. Furthermore, three epimerase (E) domains were found downstream of the modules for Ala, Ser, and Leu, which corresponded to the chemically determined absolute configurations (Figure 4b).

The biosynthetic pathways to produce the cinnamate units present in the coprisamides apparently resemble those of

skyllamycin<sup>18</sup> and atratumycin,<sup>19</sup> which also possess modified cinnamoyl moieties. Although the exact procedures and mechanisms were not determined experimentally, general biosynthetic pathways and enzyme candidates for formation of the cinnamates could be predicted based on the presence of several homologous enzymes in the coprisamide and skyllamycin gene clusters. More specifically, 10 genes in the

coprisamide C/D biosynthetic gene cluster shared high similarity to the cinnamoyl residue synthases of skylamycin (Table S4). Genes such as ketosynthase/chain length factor (*cprA–cprD*), ketoreductase (*cprJ*), dehydratase (*cprK* and *cprL*), and *cis–trans* isomerase (*cprE* and *cprN*) were speculated to compose the cinnamoyl synthetic gene cassettes, which are responsible for producing the cinnamic acid units during coprisamide biosynthesis (Figure 4c). Moreover, the cinnamoyl synthetic gene cassette was equally observed in the coprisamide A/B cluster (Figure S26 and Table S5). Again, we note that the key structural feature distinguishing coprisamides C/D from coprisamides A/B is the incorporation of modified cinnamate units. We therefore propose that isovaleryl-CoA is used as the precursor molecule instead of acetyl-CoA during the biosynthesis of coprisamides C/D.

Another unique structural feature of coprisamides is inclusion of the Dap moiety as a nonproteinogenic amino acid residue, in addition to the branched amino acid attached to Dap. This unusual Dap unit is likely generated from *O*-phosphoserine by CprF and CprG and the subsequent incorporation of an additional Val residue as the branched residue (Figure 4d). CprF and CprG share homology with 2,3-Dap synthases, namely, SbnA and SbnB, respectively, which originate from the staphyloferrin B gene cluster.<sup>20</sup> SbnA produces *N*-(1-amino-1-carboxy-2-ethyl)glutamic acid using *L*-glutamic acid and *O*-phospho-*L*-serine, and this intermediate is hydrolyzed by SbnB to yield  $\alpha$ -ketoglutarate and *L*-2,3-diaminopropanoic acid during staphyloferrin B biosynthesis. Therefore, the Dap unit of coprisamides could be synthesized in a similar manner to that used for staphyloferrin B biosynthesis. However, no gene products responsible for the subsequent process connecting an additional Val residue to 2,3-Dap were found in the coprisamide A/B or coprisamide C/D gene clusters. Therefore, we hypothesize that an unknown enzyme, located outside of the biosynthetic cluster, catalyzes incorporation of the Val residue (Figures 4d and S26).

During the functional analysis of genes from the coprisamide clusters, genes encoding glutamate mutase (methylaspartate mutase) were detected based on their translated amino acid sequences. Following a previous investigation of the glutamate-fermentation pathway in *Clostridium* spp.,<sup>21</sup> this enzyme was found to catalyze the reversible conversion of *L*-glutamic acid to 3*S*-*L*- $\beta$ -methylaspartic acid. With respect to the coprisamide C/D cluster, the methylaspartate mutases were coded discretely in two genes, namely, the large subunit (*cprP*) and the small subunit (*cprO*), which are homologous to *copP* and *copO* for coprisamides A/B.

## EXPERIMENTAL SECTION

**General Experimental Procedures.** Optical-rotation data were acquired using a JASCO P-2000 polarimeter with a 1 cm cuvette at 20 °C. Ultraviolet and circular dichroism spectra were obtained using an Applied Photophysics Chirascan-Plus circular dichroism spectrometer with a 2 mm CD cell. Infrared spectra were recorded with a JASCO FT/IR-4200 instrument. 1D and 2D NMR spectra were collected using Bruker Avance 850 and 800 MHz NMR spectrometers. LC/MS chromatographic data were acquired using an Agilent Technologies 1200 series HPLC instrument, coupled with an Agilent Technologies 6130 quadrupole MS equipped with an electrospray ionization (ESI) source. The HR-ESIMS data were measured using an AB Sciex 5600 QTOF HR-MS instrument.

**Bacterial Isolation.** Carrion beetle specimens, which were morphologically identified as *S. perforata* (Figure S27),<sup>22</sup> were collected from Gwanak Mountain, Seoul, Republic of Korea, in July 2017. To

isolate actinobacterial strains from the beetles, their guts were extracted, suspended in sterilized water, spread onto various kinds of agar media used for isolating bacteria, and incubated at 30 °C for 14 days. *Micromonospora* sp. UTJ3 was grown on potato dextrose agar medium and isolated as a single strain. Analysis of the 16S rDNA sequence of strain UTJ3 indicated that this actinobacterial strain belongs to the *Micromonospora* genus (GenBank accession no. MT312832) and shares 98% identity with *Micromonospora viridifaciens* (GenBank accession no. LT607411).

**Cultivation and Extraction.** The *Micromonospora* sp. UTJ3 strain was initially inoculated in 200 mL of YEME liquid medium (containing 4 g of yeast extract, 10 g of malt extract, and 4 g of glucose per 1 L of sterilized water) and incubated at 30 °C in a rotary shaker at 160 rpm. After 3 days, a portion (15 mL) of the bacterial culture was transferred into 1 L of modified K liquid medium (containing 2 g of yeast extract, 2 g of peptone, 2 g of glucose, 3 g of mannitol, 5 g of malt extract, 5 g of soybean peptone, and 5 g of soluble starch per 1 L of sterilized water) for scale-up. This culture stage was maintained for 7 days. The whole culture (18 L) was transferred to a separating funnel and extracted with an equivalent volume of ethyl acetate (EtOAc). The EtOAc layer was separated from the aqueous phase, dried over anhydrous sodium sulfate, and concentrated using a rotary evaporator *in vacuo* to obtain the dry extract (10 g).

**Purification of Coprisamides C and D (1 and 2).** The entire bacterial extract was dissolved in methanol (MeOH), adsorbed on Celite, and loaded onto a reversed-phase flash chromatography column (20 g of YMC C<sub>18</sub> resin, 60 × 40 mm). Various concentrations of MeOH–H<sub>2</sub>O (20%, 40%, 60%, and 100%; 200 mL) were sequentially used for fractionation. A 20  $\mu$ L aliquot of each fraction was analyzed by LC/MS, which indicated that 1 and 2 were eluted in the 100% MeOH fraction. This fraction was then subjected to semipreparative HPLC using a reversed-phase column (YMC, C<sub>18</sub>(2), 250 × 10 mm) with a gradient solvent system (40–65% CH<sub>3</sub>CN–H<sub>2</sub>O over 50 min with 0.1% trifluoroacetic acid; flow rate, 2 mL/min; detection, UV 280 nm). Coprisamides C and D (1 and 2) were eluted after 34 and 38 min, respectively. Coprisamide C (1) was repurified with a C<sub>18</sub>(2) column (Phenomenex, 250 × 4.6 mm) and eluted at a retention time of 39.5 min (9 mg) under gradient solvent conditions (30–50% CH<sub>3</sub>CN–H<sub>2</sub>O over 40 min with 0.1% trifluoroacetic acid). Coprisamide D (2) was also purified (33–53% CH<sub>3</sub>CN–H<sub>2</sub>O over 40 min with 0.1% trifluoroacetic acid) with an identical column and was obtained in its pure form after 37.5 min (2 mg).

**Coprisamide C (1):** white powder; [ $\alpha$ ]<sub>D</sub><sup>20</sup> –2 (c 0.2, MeOH); UV (MeOH)  $\lambda$ <sub>max</sub> (log  $\epsilon$ ) 267 (3.35), 288 (3.31) nm; IR (neat)  $\nu$ <sub>max</sub> 3280, 2970, 1679, 1518, 1205, 1143 cm<sup>–1</sup>; for <sup>1</sup>H and <sup>13</sup>C NMR spectral data, see Table 1; HR-ESIMS [M + H]<sup>+</sup> *m/z* 923.5242 (calcd for C<sub>47</sub>H<sub>71</sub>N<sub>8</sub>O<sub>11</sub>, 923.5237).

**Coprisamide D (2):** white powder; [ $\alpha$ ]<sub>D</sub><sup>20</sup> –1 (c 0.2, MeOH); UV (MeOH)  $\lambda$ <sub>max</sub> (log  $\epsilon$ ) 267 (3.21), 288 (3.18) nm; IR (neat)  $\nu$ <sub>max</sub> 3323, 2930, 1686, 1518, 1207, 1139 cm<sup>–1</sup>; for <sup>1</sup>H and <sup>13</sup>C NMR spectral data, see Table 1; HR-ESIMS [M + H]<sup>+</sup> *m/z* 923.5242 (calcd for C<sub>47</sub>H<sub>71</sub>N<sub>8</sub>O<sub>11</sub>, 923.5237).

**Determination of the Absolute Configurations at the  $\alpha$ -Carbon Atoms of Coprisamide C (1).** To acquire free amino acid units, coprisamide C (1) (2 mg) was dissolved in 6 N HCl (1 mL) and heated at 100 °C for 2 h. Subsequently, the hydrolysate was cooled in an ice bath (0 °C) for 5 min and rapidly vaporized *in vacuo*. To eliminate the residual HCl, deionized water (1 mL) was added to the vial and the contents were allowed to dry completely under reduced pressure; this step was repeated in triplicate. The resulting dried mixture was then lyophilized for 24 h and divided into two vials. To acquire *L*-FDAA derivatives of the amino acids, the hydrolysate in one of the vials was redissolved in 1 N NaHCO<sub>3</sub> (500  $\mu$ L) and treated with an *L*-FDAA solution (100  $\mu$ L, 10 mg/mL in acetone). The reaction mixture was stirred at 80 °C for 10 min, then quenched with 2 N HCl (250  $\mu$ L). The *D*-FDAA derivatives were obtained in a similar manner using a *D*-FDAA solution. The products were diluted with a 50 vol % CH<sub>3</sub>CN–H<sub>2</sub>O solution for LC/MS analysis [Phenomenex, C<sub>18</sub>(2), 100 × 4.6 mm; 10–60 vol % CH<sub>3</sub>CN–H<sub>2</sub>O with 0.1% formic acid over 50 min; flow

rate, 0.7 mL/min]. The retention times of the FDAA derivatives were confirmed by MS ion extraction (Figure S17).

**Determination of the Configuration at the  $\beta$ -Carbon Atom of  $\beta$ -Me-Asp in Coprisamide C (1).** The absolute configuration of the  $\beta$ -carbon atom of  $\beta$ -Me-Asp in coprisamide C (1) was assigned by performing PGME derivatization. To prepare the S-PGME amide product (1a), 1 (2 mg) was dissolved in *N,N*-dimethylformamide (500  $\mu$ L) and treated with (benzotriazol-1-yloxy)tripyrrolidino-phosphonium hexafluorophosphate (3.3 mg), 1-hydroxybenzotriazole hydrate (1.5 mg), 4-methylmorpholine (100  $\mu$ L), and S-PGME (5.0 mg). The derivatization was allowed to proceed at room temperature for 1 h prior to quenching by the addition of a 5% HCl solution (1 mL). The reaction mixture was purified using a C<sub>18</sub> column (YMC, 250  $\times$  10 mm) under gradient solvent conditions (45–75% CH<sub>3</sub>CN–H<sub>2</sub>O with 0.1% trifluoroacetic acid over 60 min). The desired product, the S-PGME amide of 1 (1a), was eluted after 54 min. The R-PGME amide of 1 (1b) was also prepared using the same method (retention time: 52.5 min under the identical HPLC conditions). The molecular formulas of 1a and 1b were deduced as C<sub>56</sub>H<sub>79</sub>N<sub>9</sub>O<sub>12</sub> via their LR-ESIMS data ([M + H]<sup>+</sup> *m/z* at 1070, [M + Na]<sup>+</sup> *m/z* at 1092, and [M – H]<sup>–</sup> *m/z* at 1068).

**S-PGME amide of 1 (1a):** <sup>1</sup>H NMR (800 MHz, CD<sub>3</sub>OD)  $\delta$  7.98 (1H, d, *J* = 15.5 Hz), 7.57 (1H, d, *J* = 7.5 Hz), 7.56 (1H, d, *J* = 7.5 Hz), 7.44–7.41 (2H, m), 7.33 (1H, dd, *J* = 7.5, 7.5 Hz), 7.32–7.30 (4H, m), 7.24 (1H, dd, *J* = 7.5, 7.5 Hz), 6.85 (1H, d, *J* = 15.5 Hz), 6.73 (1H, dd, *J* = 10.5, 10.5 Hz), 6.57 (1H, d, *J* = 10.5 Hz), 6.28 (1H, dd, *J* = 15.5, 10.5 Hz), 5.90 (1H, s), 5.88 (1H, td, *J* = 14.5, 7.5 Hz), 4.49 (1H, m), 4.47–4.43 (2H, m), 4.42 (1H, m), 4.32 (1H, d, *J* = 6.5 Hz), 4.12 (1H, d, *J* = 6.5 Hz), 3.92 (1H, dd, *J* = 11.0, 4.5 Hz), 3.77 (1H, dd, *J* = 11.0, 5.5 Hz), 3.73 (3H, s), 3.61 (1H, m), 3.33 (1H, m), 3.03 (1H, m), 2.22 (1H, m), 2.05 (2H, dd, *J* = 7.5, 7.5 Hz), 1.99 (1H, m), 1.74–1.67 (4H, m), 1.44 (3H, d, *J* = 7.5 Hz), 1.34 (3H, d, *J* = 7.5 Hz), 0.98 (3H, d, *J* = 7.0 Hz), 0.97 (3H, d, *J* = 7.0 Hz), 0.96–0.94 (6H, m), 0.93 (3H, d, *J* = 6.5 Hz), 0.93 (3H, d, *J* = 6.5 Hz), 0.92–0.88 (6H, m).

**R-PGME amide of 1 (1b):** <sup>1</sup>H NMR (800 MHz, CD<sub>3</sub>OD)  $\delta$  7.74 (1H, d, *J* = 15.5 Hz), 7.59 (1H, d, *J* = 7.5 Hz), 7.39 (1H, d, *J* = 7.5 Hz), 7.39 (1H, d, *J* = 7.5 Hz), 7.38–7.31 (3H, m), 7.29 (1H, dd, *J* = 7.5, 7.5 Hz), 7.27–7.25 (2H, m), 6.88 (1H, d, *J* = 15.5 Hz), 6.43 (1H, d, *J* = 10.5 Hz), 6.36 (1H, dd, *J* = 10.5, 10.5 Hz), 6.16 (1H, dd, *J* = 14.5, 10.5 Hz), 5.88 (1H, td, *J* = 14.5, 7.5 Hz), 5.44 (1H, s), 5.22 (1H, dd, *J* = 11.0, 1.5 Hz), 4.55 (1H, br s), 4.43–4.39 (2H, m), 4.32 (1H, dd, *J* = 9.0, 7.0 Hz), 4.27 (1H, dd, *J* = 13.5, 9.5 Hz), 4.03 (1H, m), 3.94 (1H, dd, *J* = 11.5, 1.5 Hz), 3.70 (3H, s), 3.61 (1H, d, *J* = 5.5 Hz), 3.57 (1H, br s), 3.33 (1H, m), 3.04 (1H, dd, *J* = 13.5, 5.0 Hz), 2.52 (1H, m), 2.17 (1H, m), 1.93 (2H, dd, *J* = 7.5, 7.5 Hz), 1.67 (1H, m), 1.65–1.58 (2H, m), 1.52 (1H, m), 1.43 (3H, d, *J* = 7.5 Hz), 1.10 (3H, d, *J* = 7.5 Hz), 1.08 (3H, d, *J* = 7.5 Hz), 1.04 (3H, d, *J* = 7.5 Hz), 0.99 (3H, d, *J* = 7.5 Hz), 0.97 (3H, d, *J* = 7.5 Hz), 0.94 (3H, d, *J* = 7.5 Hz), 0.92 (3H, d, *J* = 7.5 Hz), 0.87 (3H, d, *J* = 7.5 Hz), 0.87 (3H, d, *J* = 7.5 Hz).

**Resazurin Microtiter Assay against *Mycobacterium tuberculosis* mc<sup>2</sup> 6230 WT.** The MIC<sub>50</sub> values of coprisamides A–D against the Mtb mc<sup>2</sup> 6230 strain were obtained by performing REMAs. The avirulent Mtb strain was grown at 37 °C in Middlebrook 7H9 liquid medium (Difco) supplemented with 0.5% albumin, 0.2% glucose, 0.085% NaCl, 0.2% glycerol, 0.05% Tween-80, 24  $\mu$ g/mL pantothenate, and 0.2% casamino acid. Briefly, 100  $\mu$ L aliquots of the medium were added to all wells of a 96-well microtiter plate, adjusting the final bacterial OD<sub>600</sub> to 0.005. Coprisamides A–D were added to each well using a 2-fold serial-dilution method. The reference compounds, isoniazid and ethambutol, were effective against Mtb at low MIC<sub>50</sub> values of 0.03 and 0.83  $\mu$ g/mL, respectively. The prepared 96-well plates were incubated at 37 °C. After 5 days, resazurin was added to each well [0.025% (wt/vol)], and the fluorescence was read (560–590 nm) using a SpectraMax M3 multi-mode microplate reader (Molecular Devices, CA, USA). The MIC<sub>50</sub> values of the compounds were calculated based on results obtained in triplicate using Prism 6 software (GraphPad Software, Inc., La Jolla, CA, USA).

**Quinone Reductase Assay.** Hepa-1c1c7 murine hepatoma cells (American Type Culture Collection, Manassas, VA, USA) were used in this study. The QR-inducing activities of coprisamides C and D (1 and

2) were evaluated by performing microtiter assays, as previously reported.<sup>2</sup>

**Sequencing and Gene Annotation of Coprisamide-Producing Strains.** Whole-genome sequence data of the coprisamide-producing strains, *Streptomyces* sp. SNU533 and *Micromonospora* sp. UTJ3, were acquired by ChunLab, Inc. using single-molecule sequencing technology with the PacBio RS II system. The genomic sequence data were assembled using a hierarchical genome-assembly process with SMRT analysis 2.3.0, resulting in 8 935 192 bp (5 contigs) and 7 757 889 bp (1 contig) of sequence data, respectively. The DNA sequence data were annotated with EggNOG 4.5, Swiss-Prot, KEGG, and SEED, as part of ChunLab's in-house pipeline. Further analysis revealed that the genome of *Streptomyces* sp. SNU533 was composed of 71.03% G + C, 8281 coding DNA sequences (CDSs), and 67 tRNA genes. In the case of *Micromonospora* sp. UTJ3, 71.43% G + C, 6045 CDSs, and 51 tRNA genes were identified. The antiSMASH 5.0 software program was utilized to determine biosynthetic gene clusters of coprisamides. The genomic sequence data were deposited in GenBank under accession numbers MT813120 for coprisamides A and B and MT813119 for coprisamides C and D.

## ■ ASSOCIATED CONTENT

### Supporting Information

The Supporting Information is available free of charge at <https://pubs.acs.org/doi/10.1021/acs.jnatprod.0c00864>.

1D and 2D NMR spectra, HR-ESIMS spectra, and CD spectra for 1 and 2, as well as genomic analysis of *Micromonospora* sp. UTJ3 and *Streptomyces* sp. SNU533 (PDF)

## ■ AUTHOR INFORMATION

### Corresponding Author

Dong-Chan Oh – Natural Products Research Institute, College of Pharmacy, Seoul National University, Seoul 08826, Republic of Korea; [orcid.org/0000-0001-6405-5535](https://orcid.org/0000-0001-6405-5535); Phone: +82 28802491; Email: [dongchanoh@snu.ac.kr](mailto:dongchanoh@snu.ac.kr); Fax: +82 27628322

### Authors

Yern-Hyerk Shin – Natural Products Research Institute, College of Pharmacy, Seoul National University, Seoul 08826, Republic of Korea

Yeon Hee Ban – Natural Products Research Institute, College of Pharmacy, Seoul National University, Seoul 08826, Republic of Korea

Tae Ho Kim – Molecular Mechanism of Antibiotics, Division of Life Science, Research Institute of Life Science and Division of Applied Life Science (BK21plus Program), Gyeongsang National University, Jinju 52828, Republic of Korea

Eun Seo Bae – Natural Products Research Institute, College of Pharmacy, Seoul National University, Seoul 08826, Republic of Korea

Jongheon Shin – Natural Products Research Institute, College of Pharmacy, Seoul National University, Seoul 08826, Republic of Korea; [orcid.org/0000-0002-7536-8462](https://orcid.org/0000-0002-7536-8462)

Sang Kook Lee – Natural Products Research Institute, College of Pharmacy, Seoul National University, Seoul 08826, Republic of Korea; [orcid.org/0000-0002-4306-7024](https://orcid.org/0000-0002-4306-7024)

Jichan Jang – Molecular Mechanism of Antibiotics, Division of Life Science, Research Institute of Life Science, Gyeongsang National University, Jinju 52828, Republic of Korea

Yeo Joon Yoon – Natural Products Research Institute, College of Pharmacy, Seoul National University, Seoul 08826, Republic of Korea; [orcid.org/0000-0002-3637-3103](https://orcid.org/0000-0002-3637-3103)

Complete contact information is available at:

<https://pubs.acs.org/10.1021/acs.jnatprod.0c00864>

## Notes

The authors declare no competing financial interest.

## ACKNOWLEDGMENTS

This work was supported by the National Research Foundation of Korea Grants funded by the Korean Government (Ministry of Science and ICT) (2018R1A4A1021703, 2019R1A2B5B03069338, and 2020R1A2C2003518).

## REFERENCES

- (1) (a) Engle, P.; Moran, N. A. *FEMS Microbiol. Rev.* **2013**, *37*, 699–735. (b) Ramadhar, T. R.; Beemelmanns, C.; Currie, C. R.; Clardy, J. J. *Antibiot.* **2014**, *67*, 53–58.
- (2) Um, S.; Park, S. H.; Kim, J.; Park, H. J.; Ko, K.; Bang, H.-S.; Lee, S. K.; Shin, J.; Oh, D.-C. *Org. Lett.* **2015**, *17*, 1272–1275.
- (3) Guo, H.; Benndorf, R.; Lechnitz, D.; Klassen, J. L.; Vollmers, J.; Görls, H.; Steinacker, M.; Weigel, C.; Dahse, H.-M.; Kater, A.-K.; de Beer, Z. W.; Poulsen, M.; Beemelmanns, C. *Chem. - Eur. J.* **2017**, *23*, 9338–9345.
- (4) Um, S.; Bach, D.-H.; Shin, B.; Ahn, C.-H.; Kim, S.-H.; Bang, H.-S.; Oh, K.-B.; Lee, S. K.; Shin, J.; Oh, D.-C. *Org. Lett.* **2016**, *18*, 5792–5795.
- (5) (a) Shin, Y.-H.; Beom, J. Y.; Chung, B.; Shin, Y.; Byun, W. S.; Moon, K.; Bae, M.; Lee, S. K.; Oh, K.-B.; Shin, J.; Yoon, Y. J.; Oh, D.-C. *Org. Lett.* **2019**, *21*, 1804–1808. (b) Shin, Y.-H.; Kang, S.; Byun, W. S.; Jeon, C.-W.; Chung, B.; Beom, J. Y.; Hong, S.; Lee, J.; Shin, J.; Kwak, Y.-S.; Lee, S. K.; Oh, K.-B.; Yoon, Y. J.; Oh, D.-C. *J. Nat. Prod.* **2020**, *83*, 277–285.
- (6) Shin, B.; Park, S. H.; Kim, B.-Y.; Jo, S.-I.; Lee, S. K.; Shin, J.; Oh, D.-C. *J. Nat. Prod.* **2017**, *80*, 2910–2916.
- (7) Hong, S.-H.; Ban, Y. H.; Byun, W. S.; Kim, D.; Jang, Y.-J.; An, J. S.; Shin, B.; Lee, S. K.; Shin, J.; Yoon, Y. J.; Oh, D.-C. *J. Nat. Prod.* **2019**, *82*, 903–910.
- (8) Kaltenpoth, M.; Steiger, S. *Mol. Ecol.* **2014**, *23*, 1251–1267.
- (9) Dekeirsschietter, J.; Verheggen, F.; Lognay, G.; Haubruge, E. *Biotechnol. Agron. Soc. Environ.* **2011**, *15*, 435–447.
- (10) Shin, Y.-H.; Bae, S.; Sim, J.; Hur, J.; Jo, S.-I.; Shin, J.; Suh, Y.-G.; Oh, K.-B.; Oh, D.-C. *J. Nat. Prod.* **2017**, *80*, 2962–2968.
- (11) Meinwald, J.; Roach, B.; Eisner, T. *J. Chem. Ecol.* **1987**, *13*, 35–38.
- (12) Meinwald, J.; Roach, B.; Hicks, K.; Alsop, D.; Eisner, T. *Experientia* **1985**, *41*, 516–519.
- (13) Ito, N.; Katoh, T.; Kobayashi, N.; Katakura, H. *Zool. Sci.* **2010**, *27*, 313–319.
- (14) Ikeda, H.; Kagaya, T.; Kubota, K.; Abe, T. *Evolution* **2008**, *62*, 2067–2079.
- (15) Fujii, K.; Ikai, Y.; Oka, H.; Suzuki, M.; Harada, K. *Anal. Chem.* **1997**, *69*, 5146–5151.
- (16) Yabuuchi, T.; Kusumi, T. *J. Org. Chem.* **2000**, *65*, 397–404.
- (17) Blin, K.; Shaw, S.; Steinke, K.; Villebro, R.; Ziemert, N.; Lee, S. Y.; Medema, M. H.; Weber, T. *Nucleic Acids Res.* **2019**, *47*, W81–W87.
- (18) (a) Toki, S.; Agatsuma, T.; Ochiai, K.; Saitho, Y.; Ando, K.; Nakanishi, S.; Lokker, N. A.; Giese, N. A.; Matsuda, Y. *J. Antibiot.* **2001**, *54*, 405–414. (b) Pohle, S.; Appelt, C.; Roux, M.; Fiedler, H.-P.; Süßmuth, R. D. *J. Am. Chem. Soc.* **2011**, *133*, 6194–6205.
- (19) Sun, C.; Yang, Z.; Zhang, C.; Liu, Z.; He, J.; Liu, Q.; Zhang, T.; Ju, J.; Ma, J. *Org. Lett.* **2019**, *21*, 1453–1457.
- (20) Kobylarz, M. J.; Grigg, J. C.; Takayama, S. J.; Rai, D. K.; Heinrichs, D. E.; Murphy, M. E. P. *Chem. Biol.* **2014**, *21*, 379–388.
- (21) Barker, H. A.; Rooze, V.; Suzuki, F.; Iodice, A. A. *J. Biol. Chem.* **1964**, *239*, 3260–3266.
- (22) Cho, Y. B.; Choi, S.-W.; Nishikawa, M.; Kwon, Y. J. *Korean J. Syst. Zool.* **2004**, *20*, 63–71.